

## Evaluating and Monitoring Methods of HVDC Valve Radiator Blockage Based on Applied Heat Transfer

Li Zhang<sup>1</sup>, Mingxing Li<sup>1</sup>, Fan Yang<sup>1, \*</sup>, Wenzhen Li<sup>2</sup>, Hailong Zhang<sup>2</sup>, and Songlin Liu<sup>1</sup>

**Abstract**—Valve radiator blockage is a serious problem endangering the safety of thyristor. At present, there are no effective methods for blockage evaluation and monitoring. This paper analyzes the heat dissipation state of a radiator under different blocking conditions and divides it into abnormal heat dissipation and normal heat dissipation. Then, based on reliability theory, the tolerance index  $\psi$  for blockage and the probability index  $\theta$  for overheating are proposed to evaluate the blockage hazard of the thyristor. Also, the thermal circuit model of the valve group is established to monitor radiator blockage. According to the model, the corresponding relationship between radiator blockage and valve temperature distribution is solved, and the blockage detects index  $\langle W \rangle$  based on device temperature is given to judge radiator block. Through the infrared monitoring temperature solution,  $\langle w \rangle$  judgment of radiator blockage is consistent with the set blockage.

### 1. INTRODUCTION

A cooling water system is designed in an HVDC valve for thyristor cooling. The system scaling easily blocks the radiator, thus affecting the radiator heat dissipation and endangering the safety of the valve.

At present, many scholars have studied cooling water system scaling. For example, Jackson and Abrahamsson found that aluminium oxide was the main component of scaling on voltage sharing electrodes [1]. A team in North China Electric Power University investigated the severity of scaling impact. The survey showed that more than 66% of the valve failures were related to scaling [2, 3]. A team in North China Electric Power University analyzed the radiators' corrosion rate with Faraday's Law and found that scaling layer produced by converter valves was about 2.5 kg/year [3]. Xu proposed to evaluate the corrosion and scaling of a valve cooling system through the online monitoring of cooling water quality [4]. Jiang et al. considered the structure of a valve cooling system and used the fault tree analysis method to establish a reliability model of the HVDC valve cooling system [5]. Yang et al. proposed that the fault analysis and diagnosis of the valve cooling system can be realized by collecting the operation condition of the valve cooling system and analyzing and processing the operation condition information [6]. Ding et al. found that the growth of scale thickness was more than 0.295 mm every year, and scaling layer was easy to fall off during cleaning [7]. Many related literatures mentioned that radiator blockage had serious harm to torque converter valve [4–9]. The method used in engineering was to judge whether the valve block is blocked or not according to the threshold value of the valve block temperature. In contrast, the threshold value method can only identify the thermal blockage when the blockage is serious. However, there is a lack of a suitable method to evaluate and monitor all cases of radiator blockage.

This paper aims to evaluate the harm caused by radiator blockage and gives an online monitoring method. On the one hand, by the simulation of the valve group, the temperature changes of the valve

---

Received 21 April 2021, Accepted 23 June 2021, Scheduled 13 August 2021

\* Corresponding author: Fan Yang (yangfancqu@gmail.com).

<sup>1</sup> State Key Laboratory of Power Transmission Equipment & System Security and New Technology, School of Electrical Engineering, Chongqing University, China. <sup>2</sup> State Grid East Inner Mongolia Electric Power Maintenance Company, Tongliao, China.

group under different blockage conditions are given. Based on the reliability analysis theory, the risk index of the valve is proposed to evaluate the overheating risk of blockage. On the other hand, the equivalent thermal circuit model of the valve group is constructed, and the Newton cooling formula is used to derive the evaluation method of radiator blockage. This monitoring method does not need to power off or dismantle the radiator. It can even directly identify the radiator blockage through the existing infrared equipment in the converter station.

## 2. EVALUATING OF RADIATOR BLOCKAGE

Fig. 1 shows the schematic diagram of the valve layer model. The green pipe is the water inlet pipe, and the blue pipe is the water outlet pipe. Each valve group is composed of 6 thyristors and 7 radiators, and the radiators cool each thyristor at the left and right ends. The cooling water flows into the radiator from the inlet pipe. It then flows out from the outlet pipe after passing through the radiator cooling channel to complete the heat dissipation process. Therefore, once the water pipe is blocked, its heat dissipation capacity will be affected [10–13].

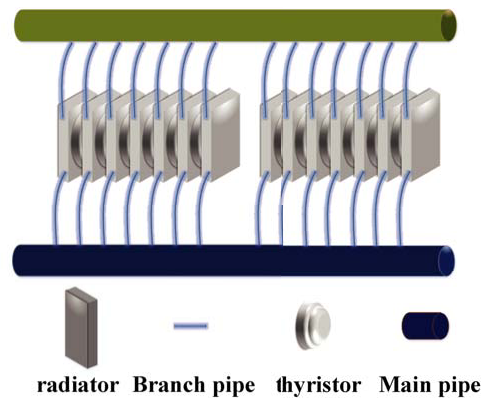


**Figure 1.** Valve layer model.

Scaling may occur on the electrodes inside the cooling system. However, the water channel inside the radiator is thin. If the electrodes scale drops out, the cooling water channel of the radiator will be blocked [14–16, 31–33].

### 2.1. Temperature and Flow Simulation of Radiator Plug

#### 1) Geometric model of radiator

Figure 2(a) shows the internal structure of the radiator. The radiator is a square with a side length of 300 mm, and its thickness is 40 mm. The cross-section of the water channel inside the radiator is a

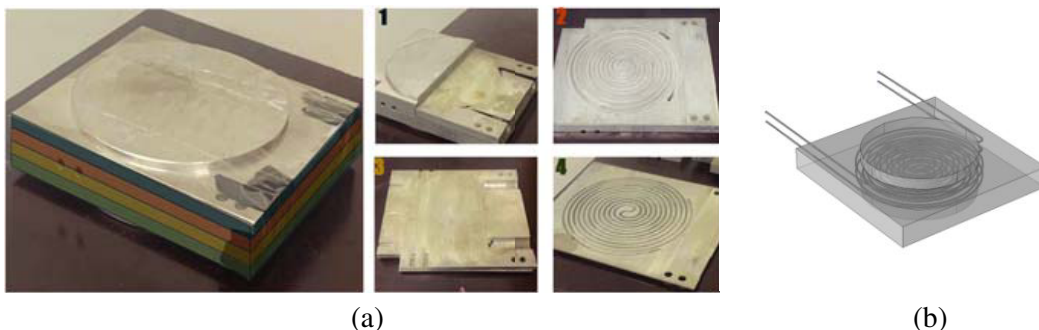


**Figure 2.** Geometric model of radiator.

square with a side length of 2 mm, divided into two water channels.

Add half thyristors on both sides of the radiator to establish a geometric model, as shown in Fig. 2(b).

## 2) Governing equations and physical parameters

### ① Flow field

The control equation of the flow field is obtained using the law of conservation of momentum and the law of conservation of mass. The temperature at the inlet is 28°C, and the temperature at the outlet is 31°C. It is considered that the density of internal cooling water does not change [17–19]. Therefore, the governing equations can be listed, such as formula (2.1) and (2.2)

$$\rho \frac{dv}{dt} = \rho F + \nabla \left( -p - \frac{2}{3} \mu \nabla \cdot v \right) + \nabla(2\mu S) \quad (2.1)$$

$$\rho \nabla v = 0 \rightarrow \nabla v = 0 \quad (2.2)$$

where  $S$  is the deformation rate tensor,  $p$  the pressure,  $v$  the velocity of fluid flow,  $\rho$  the density of the fluid, and  $\mu$  the dynamic viscosity coefficient.

### ② Temperature field

The primary forms that affect the temperature distribution are heat conduction and heat convection for the temperature field. The heat transfer of radiator and thyristor conforms to the Fourier heat conduction law. The temperature change can be described by the heat conduction formula (2.3) [17–19, 22, 26]:

$$\lambda \nabla^2 T + H(x, y, z) = 0 \quad (2.3)$$

where  $H$  is the size of the heat source in the region,  $\lambda$  the thermal conductivity of the material in the region, and  $T$  the temperature.

### ③ Physical parameters

The physical parameters include the density of water, the specific heat at constant pressure, the dynamic viscous coefficient, and the thermal conductivity of materials in the temperature field control equation and are shown in Table 1.

**Table 1.** Physical parameters.

	Density (kg/m <sup>3</sup> )	Dynamic viscosity (Pa × s)	heat conductivity (W/(m × K))	isopiestic specific heat (J/(kg × K))
Water	1 × 10 <sup>3</sup>	8.5 × 10 <sup>-4</sup>	0.61	4180
Radiator	2.7 × 10 <sup>3</sup>	-	237	880
thyristor	2.33 × 10 <sup>3</sup>	-	147	700

## 3) Boundary conditions

### ① Pressure boundary conditions

According to the structure of the HVDC valve tower, as shown in Fig. 3, the pressure difference between the inlet and outlet of the radiator can be calculated.

The pressure difference between the inlet valve and outlet valve comes from the height  $h$  of the high water tank or the water pump. According to the test data, the pressure at the inlet valve side is  $P_1 = 0.79$  Mpa, and the pressure at the outlet valve side is  $P_2 = 0.35$  Mpa. The pressure difference is shown in the formula (2.4).

$$\Delta P = P_1 - P_2 \quad (2.4)$$

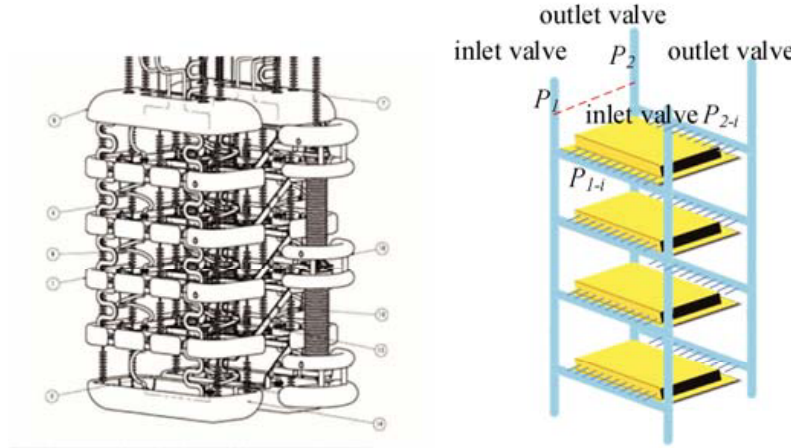


**Figure 3.** Schematic diagram of water channel of converter valve.

According to Bernoulli's principle, the pressure difference between the two sides of any valve layer should meet formula (2.5)

$$P_{1-i} - P_{2-i} = (P_1 + \rho gh_i) - (P_2 + \rho gh_i) + \frac{1}{2} \rho (v_{1-i}^2 - v_{2-i}^2) \quad (2.5)$$

In this formula,  $g$  is the acceleration of gravity,  $\rho$  the density of cooling water,  $P_{1-i}$  the pressure at layer  $i$  inlet pipe side,  $P_{2-i}$  the pressure at layer  $i$  outlet pipe side,  $v_{1-i}$  the inflow velocity of valve layer,  $v_{2-i}$  the outflow velocity of valve layer, and  $h_i$  the depth from  $I$  valve layer to the water surface.

Because the water flows in and out of the valve layer are the same, and the inlet and outlet pipes radii are the same,  $v_{1-i} = v_{2-i}$  is available. Therefore, according to formula (2.5), it can be concluded that the pressure difference at the two ends of the  $i$  valve layer radiator satisfies  $P_1 - P_2 = P_{1-i} - P_{2-i}$ .

## ② Flow field wall boundary

According to the boundary layer theory, the geometry of the model satisfies the macroscopic condition. Therefore, the boundary between water and aluminium radiator is set as a wall no-slip boundary condition.

$$v_s = 0 \quad (2.6)$$

$v_s$  is the water flow velocity on the radiator wall.

## ③ Convective heat transfer boundary of temperature field

There are four kinds of convection heat transfer on the surface of the radiator:

- A.  $h_1$  is the natural convection heat transfer coefficient above the air outer flat plate;
- B.  $h_2$  is the natural convection heat transfer coefficient below the air outer flat plate;
- C.  $h_3$  is the natural convection heat transfer coefficient of the air outer vertical flat plate;
- D.  $h_4$  is the convection heat transfer coefficient of the water cooling inside the pipe.

According to formulas (2.7), (2.8), (2.9), (2.10), the Nusselt number  $Nu$  of different boundary heat transfer can be calculated. The Nusselt number of the horizontal plate outside the air is in accordance with formula (2.7) [18, 22, 37]:

$$Nu = C(Gr \cdot Pr)^n \quad (2.7)$$

In the equation, the coefficient  $C = 0.54$ ,  $n = 1/4$  for horizontal hot side up,  $C = 0.15$ ,  $n = 1/3$  for horizontal cold side down, and  $C = 0.24$ ,  $n = 1/4$  for cold side up and hot side down.

The Nusselt number of the natural convection heat transfer coefficient of a slightly vertical plate outside the air conforms to Churchill’s and Chu’s formula (2.8):

$$Nu = \frac{h_m L}{\lambda_w} = \left\{ 0.825 + \frac{0.387 (Gr_m Pr_m)^{1/6}}{\left[ 1 + (0.492 / Pr_m)^{9/16} \right]^{8/27}} \right\}^2 \tag{2.8}$$

The convective heat transfer in the tube satisfies the Gnielinski correlation (2.9):

$$Nu = \frac{(f/8) (Re_f - 1000) Pr_f}{1 + 12.7 \sqrt{f/8} (Pr_f^{2/3} - 1)} \tag{2.9}$$

where Gr is the Grashov number of the fluid,  $\lambda_w$  the thermal conductivity of the cooling water, Re the Reynolds number of the cooling water, and Pr the Prandtl number of the fluid.

According to formula (2.10), the convective heat transfer coefficients  $h_1, h_2, h_3, h_4$  are solved.

$$h = \frac{Nu \cdot \lambda_w}{L} \tag{2.10}$$

In particular, if the cooling channel of the radiator is blocked, the cooling water velocity will be significantly affected, resulting in the convection heat transfer coefficient  $h_4 \approx 0$  between the radiator and cooling water. When the convective heat transfer coefficient is known, the boundary conditions of convective heat transfer among the radiator, thyristor, water, and air can be described by Newton’s heat transfer law.

$$q = h(T - T_0) \tag{2.11}$$

$T_0$  is the reference temperature of the heat exchange medium;

$q$  is the heat flux flowing out of the boundary.

#### 4) Simulation results

##### ① Heat dissipation analysis of single radiator

Through the simulation, the heat dissipation of the radiator after the normal operation, blocking one channel and blocking two channels is calculated, as shown in Fig. 4.

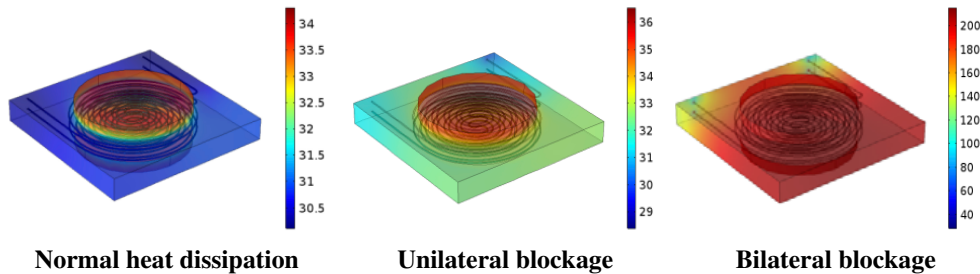


**Figure 4.** Temperature field distribution of single radiator.

According to the simulation results, the temperature difference is only 2°C when the water pipe is blocked. This state still meets the heat dissipation requirements of the converter valve. The radiator is in a potential failure state; when both ends of the radiator are blocked, the radiator’s temperature rises sharply [20–23].

##### ② Heat dissipation analysis of valve group

There are 7 radiators and 14 cooling channels in the valve group, and the blockage of the radiator in the valve group is more complicated. In order to analyze the temperature distribution of the valve group

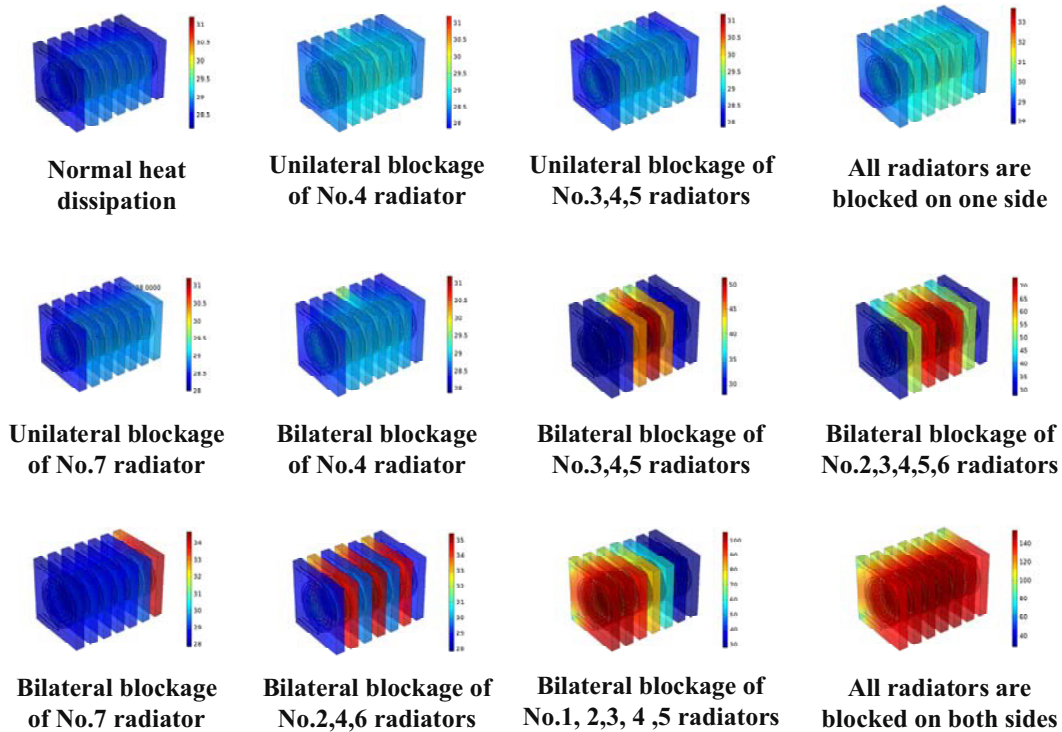


**Figure 5.** Temperature distribution of radiator under different clogging conditions.

under different blocking conditions, the simulation sets different blocking conditions for temperature field simulation analysis. The results are shown in Fig. 5.

According to the simulation results, with the increasing blockage of the radiator, the temperature of the radiator increases gradually:

A. Two radiators cool each thyristor, and each radiator has two cooling channels. This design improves the safety of the radiator. Therefore, there is only one channel blockage or other slight blockages, which causes the temperature rise of the valve group as a whole is not apparent;

B. The influence of single radiator bilateral blockage on temperature is more significant than that of two radiators blocking one channel.

C. The influence of the adjacent radiator blockage on the hot spot temperature is more significant than that of the non-adjacent radiator.

Although the cooling water channel of the radiator is partially blocked, the temperature rise will not reach the threshold given in the actual operation. However, the blockage of the radiator does occur. In this case, the cooling system is in a potentially dangerous state.

## 2.2. Evaluation Method of Blockage Hazard

There are two channels for each radiator, so there are 14 channels for one valve group. Among them, each cooling water channel has two states: blocked and not blocked. In order to measure the harm of blocking the radiator, the structure function is used to describe the failure of the radiator, and the evaluation theory of heat dissipation reliability is given.

### 1) Structure function

① Function independent variable — blocking vector

The independent variable of the structure function  $\varphi$  is a vector, and its length is 14. Each element corresponds to a channel. If the water channel is blocked, the element is 0; otherwise, it is 1.

Formula (2.12) is as follows [24, 25]:

$$a_i = \begin{cases} 1, & \text{If the } i\text{-th channel is not blocked} \\ 0, & \text{If the } i\text{-th channel is blocked} \end{cases} \quad i = 1, 2, \dots, 14 \quad (2.12)$$

For example, there are 14 channels shown in Fig. 6, of which the blue channel is blocked, and the rest are not blocked. Then  $A = (1, 1, 0, 1, 1, 1, 0, 1, 1, 1, 1, 1, 1, 1)$ .

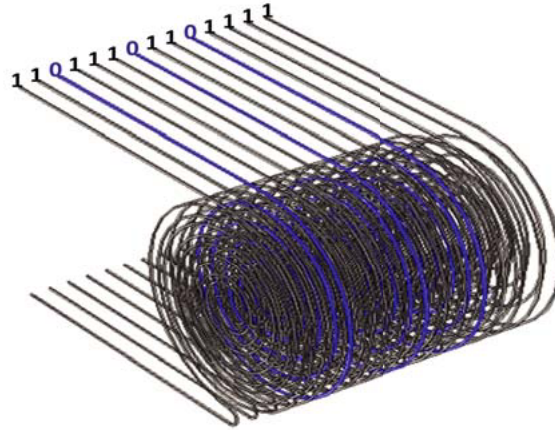


**Figure 6.** Schematic diagram of waterway blockage.

② Function dependent variable — thermal state

Using function  $\varphi(A)$  indicates the heat dissipation status of the valve group. The structure function is defined in Equation (2.13)

$$\phi_i = \begin{cases} 1, & \text{The hot spot temperature of valve group does not exceed } 70^\circ\text{C} \\ 0 & \text{The hot spot temperature of valve group exceeds } 70^\circ\text{C} \end{cases} \quad (2.13)$$

The function shows that if the hot spot temperature is less than  $70^\circ\text{C}$ , the current heat exchanger state is considered a reliable heat dissipation state. When the hot spot temperature exceeds  $70^\circ\text{C}$ , it is the fault heat dissipation state.

③ Monotonicity of functions

As the radiator water channel is constantly blocked, the heat dissipation state of the valve group will not get better. Therefore, there is a monotonous relationship between the failure of the valve group and the blockage of the radiator. It can be expressed as a formula.

$$A_1 - A_2 = (b_1, b_2, \dots, b_{14}) \quad (2.14)$$

$$\forall b_i > 0 \rightarrow \phi(A_2) \leq \phi(A_1) \quad i = 1, 2, \dots, 14 \quad (2.15)$$

**2) Hazardous state measurement**

Although the temperature of the HVDC valve group does not exceed  $70^\circ\text{C}$ , it will not cause a warning of the temperature measurement system. However, there is no guarantee that there is no blockage inside the radiator. The radiator is blocked, but the temperature measurement system cannot reach the alarm condition of the blocking state which is called the potentially dangerous state.

As shown in Fig. 7, each blocking state is represented by a box, and the transfer of blocking state from left to right is blocking 0 ~ 14 water cooling channels, respectively. The part drawn by brown dots can represent the monotonicity of the function, and the part drawn by blue dots can represent the alarm action vector. The tolerance  $\psi$  is defined according to the transfer number of action vectors. The following is the mathematical expression of hazard assessment indicators:

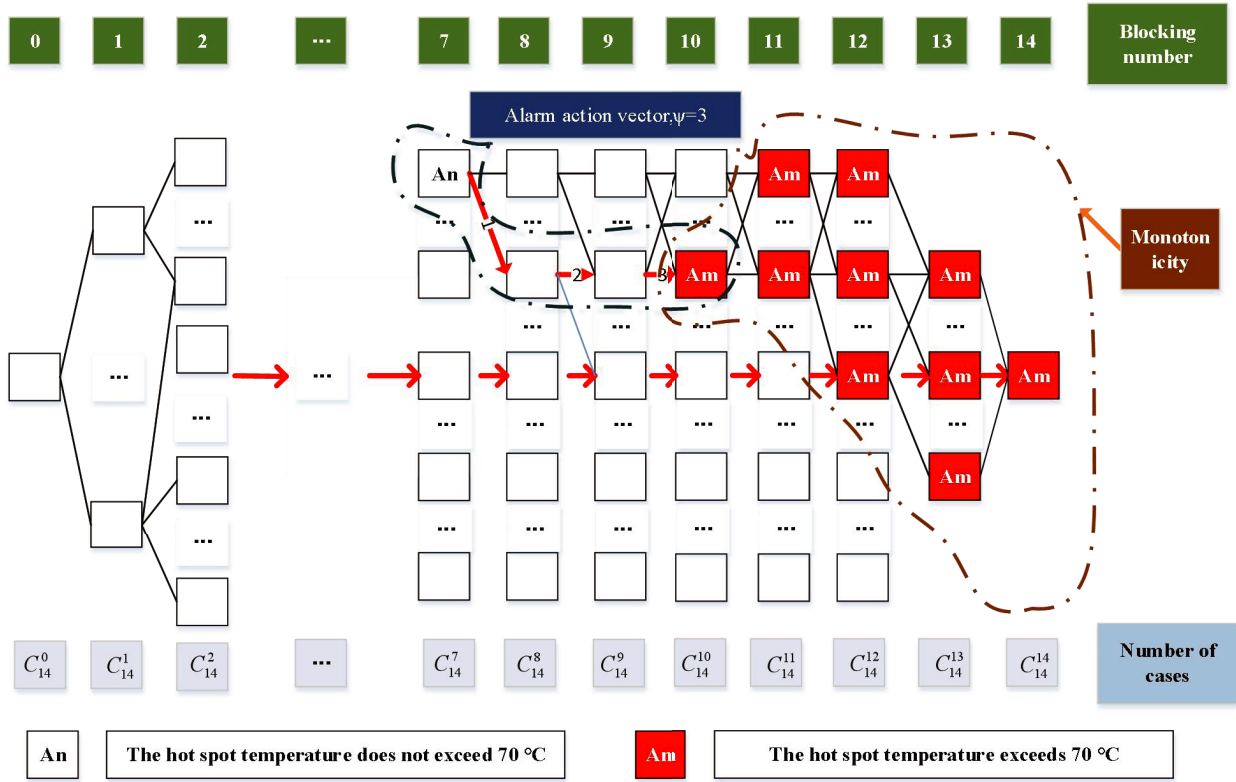


**Figure 7.** Schematic diagram of evaluation method.

① Alarm action vector

For radiator blockage, the condition of triggering alarm action should be: from state to state  $\varphi(A_i) = 1$  jumps to  $\varphi(A_j) = 0$ . The set  $M$  composed of all  $A_j$  is called the most alarm set, and the element is denoted as  $A_m$ . For the current blocking state  $A_n$ , the blocking action vector that jumps to the alarm is  $p(m)$ . The scaling action vector  $p(m)$  can be calculated by formula (2.16)

$$P(m) = \overline{A_m} \cap A_n = (\overline{a_{m1}} \cap a_{n1}, \overline{a_{m2}} \cap a_{n2}, \dots, \overline{a_{m14}} \cap a_{n14}) \quad (2.16)$$

$\cap$  is and operation algorithm.

$\overline{A}$  is  $A$  logical NOT operation.

The meaning of scaling action vector,  $p(m)$ , makes  $\varphi(A_n - p(m)) = 0$ . It means that an action such as  $p(m)$  will cause a high-temperature alarm.

② Tolerance index  $\psi$

For the blocking condition of state  $A_n$ , the minimum number of blockages from which the high-temperature alarm is caused is the standard to measure the tolerance of the current state to blockages. It can be expressed as  $\psi$  in formula (2.17)

$$\Psi = \min (\|\overline{A_n} \cap A_m\|_1) \quad m = 1, 2, \dots, q \quad (2.17)$$

The higher the index of  $\psi$  is, the better the tolerance of blockage is. If the radiator jam is calculated  $\psi = 1$ , then the valve group may overheat if another branch is blocked.

③ Possibility index  $\theta$

The possibility of heat dissipation failure due to blocking  $\psi$  root can be described by the index  $\theta$ . As in formula (2.18):

$$\theta = \text{Num} (\| \overline{A_n} \cap A_m \|_1 = \Psi) \tag{2.18}$$

The higher the  $\theta$  index is, the greater the possibility of failure of heat dissipation is.

### 3. ONLINE JUDGMENT METHOD OF RADIATOR BLOCKAGE

It is difficult to distinguish if the radiator is blocked by temperature measurement alone because of the radiator double channel cooling of the valve group, so the dangerous state of the radiator cannot be evaluated.

#### 3.1. Judgement Theory of Radiator Blockage

As shown in Fig. 8, the heat exchange of the radiator is equivalent by thermoelectric analogy, and a one-dimensional cooling path model of the valve group is established [27–30, 34–36].

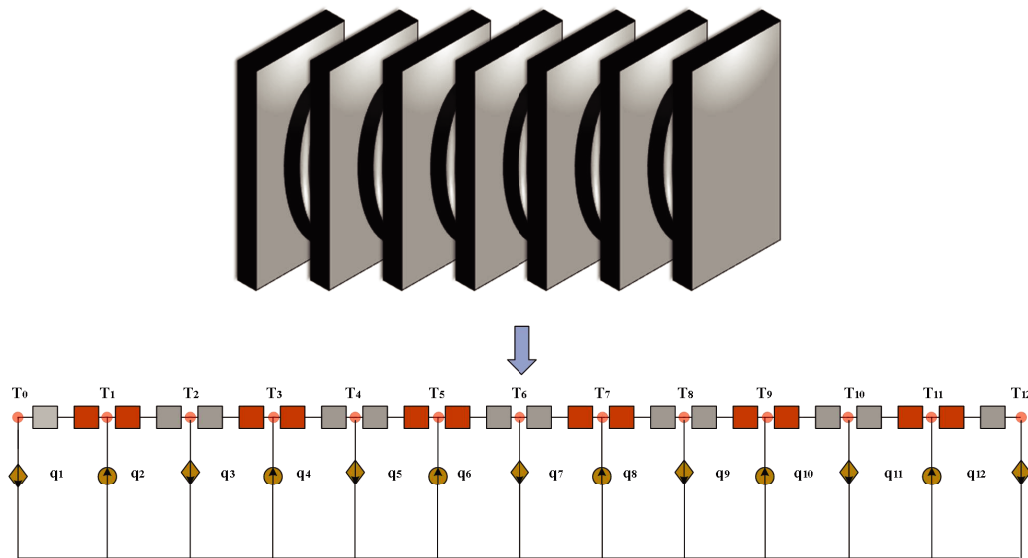


**Figure 8.** One dimensional heat circuit model of valve group.

The model is a steady-state model. According to the heat path model, the heat resistance between any two radiators is the heat resistance of 1/2 radiator  $R_{Al}$  plus 1/2 thyristor  $R_{Tr}$ . Because the model satisfies the law of conservation of capacity and the law of Fourier heat conduction, an equations can be written for the model red node as follows (3.1):

$$q_i = \frac{(2 \times T_i - T_{i+1} - T_{i-1})}{R_{Al} + R_{Tr}} \tag{3.1}$$

$T_i$  is the temperature of the red node;

$q_i$  is the inflow heat of the branch.

The second-order central difference  $U$  of device temperature is expressed as formula (3.2). The ratio of heat dissipation of different branches is equal to that of the second-order difference of corresponding node temperature, as shown in formula (3.3).

$$U_i = (2 \times T_i - T_{i+1} - T_{i-1}) \tag{3.2}$$

$$q_i : q_j = U_i : U_j \tag{3.3}$$

$i, j$  is the corresponding node or branch number.

It is also because the heat loss of the radiator can be expressed by Newton's heat transfer formula, such as formula (3.20):

$$q = h(T_{Al} - T_{water}) \cdot S \quad (3.4)$$

where  $S$  is the surface area where the radiator contacts water,  $h$  the convective heat transfer coefficient,  $T_{Al}$  the temperature of the aluminium radiator, and  $T_{water}$  the temperature of water.

The difference between before and after Blockage is that the flow rate affects the convective heat transfer coefficient  $h$  differently. The heat exchange of one channel of the radiator was  $H^1$ , and the other channel was  $H^2$ . For the value ratio of heat dissipation efficiency of radiator  $i$  and  $j$ , the equation can be derived from Eq. (3.5).

$$\frac{S}{2} \cdot (H_i^1 + H_i^2) : \frac{S}{2} \cdot (H_j^1 + H_j^2) = \frac{q_i}{T_{Al-i} - T_{water}} : \frac{q_j}{T_{Al-j} - T_{water}} \quad (3.5)$$

Formula (3.4) is brought into (3.5) which can get the ratio of radiator efficiency  $W$ , such as formula (3.6).

$$W_i : W_j = (H_i^1 + H_i^2) : (H_j^1 + H_j^2) = \frac{(2 \times T_i - T_{i+1} - T_{i-1})}{T_{Al-i} - T_{water}} : \frac{(2 \times T_j - T_{j+1} - T_{j-1})}{T_{Al-j} - T_{water}} \quad (3.6)$$

According to Equation (3.6), the heat dissipation efficiency of radiators can be obtained from thermometric data of individual devices. To make it easier to compare the heat dissipation efficiency of the 7 radiators across valve sets,  $W$  is normalized utilizing Eq. (3.7):

$$\langle W_i \rangle = \frac{W_i}{W_{max}} \quad (3.7)$$

$W_{max}$  is the maximum of all radiators in  $W$ .

### 3.2. Verification of Method Based on Simulation

Based on the simulated temperature distribution data of the valve module, the heat dispersion efficiency is brought into formula (3.7) to solve the heat transfer efficiency of the radiator and then to judge the blockage of the radiator. The validity of the theory is verified by comparing the results with the faults set by the simulation. We will analyze four scenarios:

#### 1) The radiator dissipates the heat normally

As shown in Fig. 9, the maximum surface temperature difference of the device is  $2^\circ\text{C}$  when it normally dissipates heat. Temperature distribution appears with high middle-end and low end. At the same time, as can be seen from the column chart, the heat transfer efficiency of all radiators is greater than 95%.

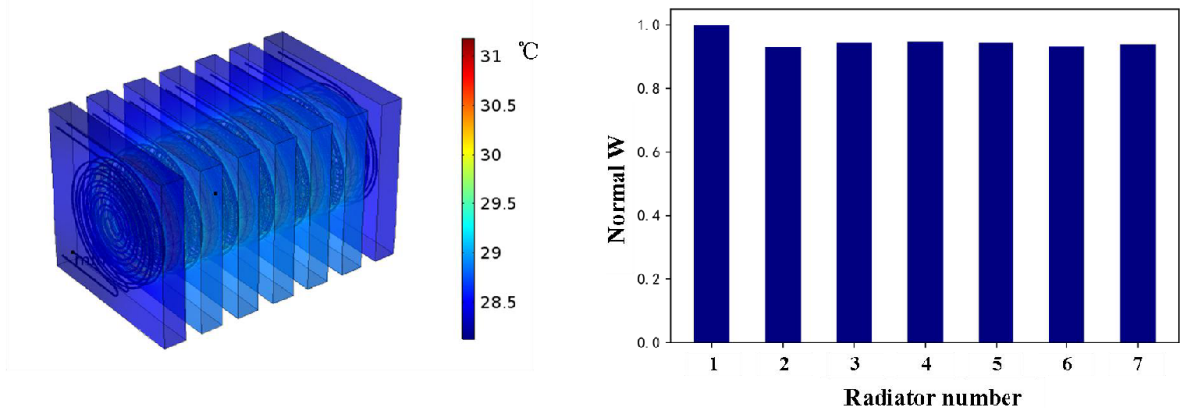


**Figure 9.** Temperature field and heat dissipation efficiency of the normal radiator.

### 2) Unilateral blockage of No. 7 radiator

As shown in Fig. 10, according to the histogram on the right, the lowest heat dissipation efficiency of the No. 7 radiator is only 37% of the maximum efficiency radiator. It can be seen that a branch of the No. 7 radiator is blocked, and the heat dissipation efficiency is reduced by less than half of the original.

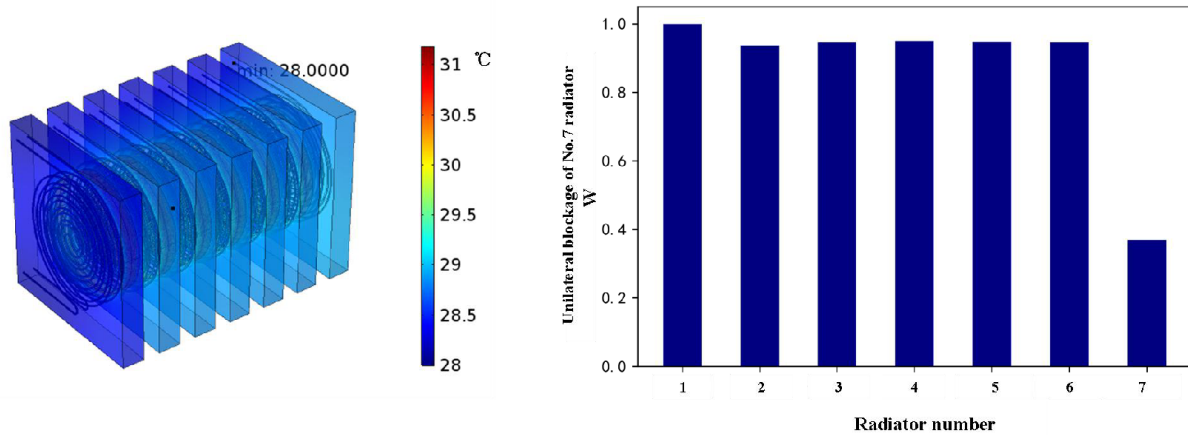


**Figure 10.** Temperature field and heat dissipation efficiency of Unilateral blockage of No. 7 radiator.

### 3) Bilateral blockage of No. 2, No. 4 and No. 6 radiators

From the observation of temperature, it can be preliminarily judged that No. 2, No. 4, and No. 6 radiators are blocked. However, whether the other radiators are blocked and whether No. 2, No. 4, and No. 6 radiators are blocked unilaterally or bilaterally cannot be determined by temperature monitoring.

As shown in Fig. 11, according to the histogram on the right, the heat dissipation efficiency of No. 2, 4, 6 radiators is close to 0, and the heat dissipation efficiency of other radiators is more than 90%.

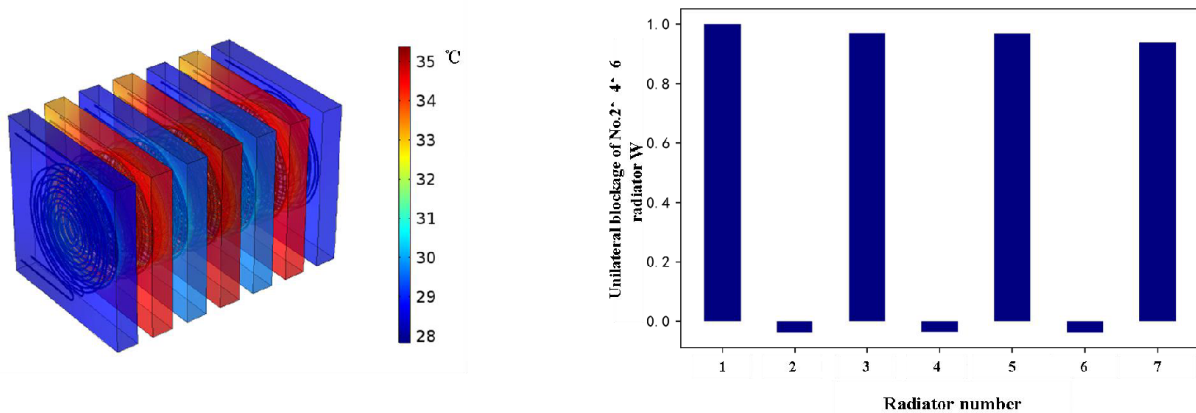


**Figure 11.** Distribution of blocking temperature field and heat dissipation efficiency of No. 2, 4, 6 radiator.

### 4) Mixed blockage

As shown in Fig. 12, two side blockage of No. 2, No. 4, and No. 6 radiators and one side blockage

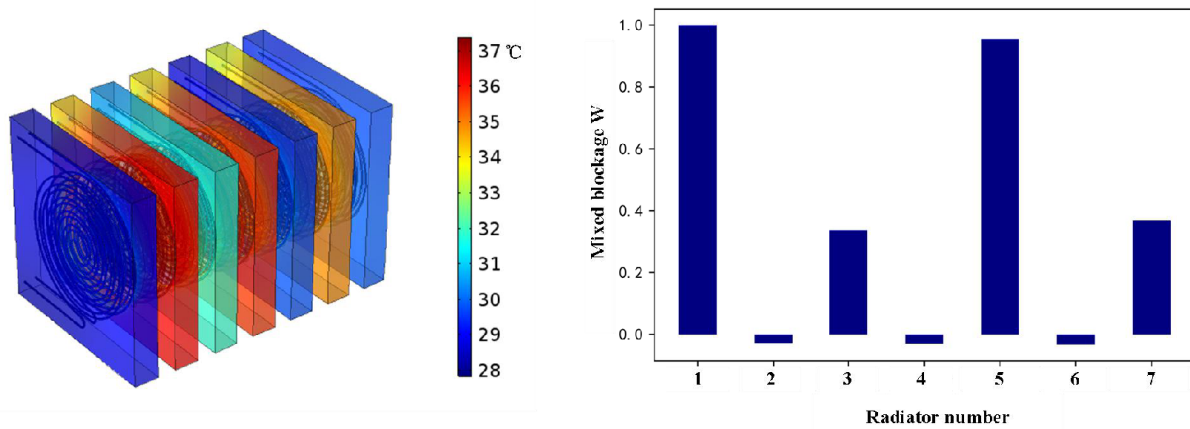


**Figure 12.** Distribution of blocking temperature field and heat dissipation efficiency of mixed blockage.

of No. 3 and No. 7 radiators are set. According to the histogram, the heat dissipation efficiency of radiators 2, 4, and 6 is almost 0, and that of radiators 3 and 7 is more than 40%.

In conclusion, the monitoring theory can be given: when both sides of the radiator are blocked, the heat dissipation efficiency of the radiator is between 0 and 0.3; when one side of the radiator is blocked, the heat dissipation efficiency of the radiator is between 0.3 and 0.8; when the radiator is blocked, the heat dissipation efficiency of the radiator is above 0.8.

Therefore, according to the temperature of the radiator and thyristor, the blockage can be judged according to Table 2.

**Table 2.** Judgment of blockage.

Blockage	Not blocked	Unilateral blockage	Bilateral blockage
Index	0.8–1	0.3–0.8	0–0.3

### 3.3. Blockage Monitoring Experiment

In order to verify the feasibility of the above-mentioned monitoring method of radiator blockage in a valve cooling system, an experimental platform of radiator blockage in the valve cooling system is built, as shown in Fig. 13, including water-cooled aluminium radiators, waterpumps, DC power supply, 8 mm

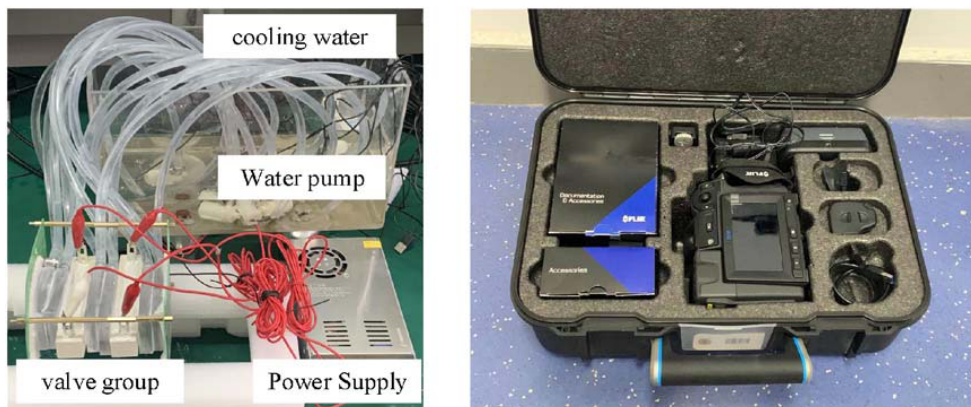


**Figure 13.** Radiator heat dissipation monitoring experimental platform.

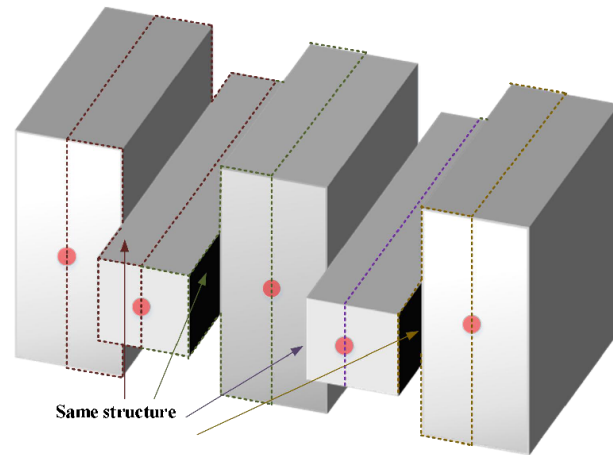
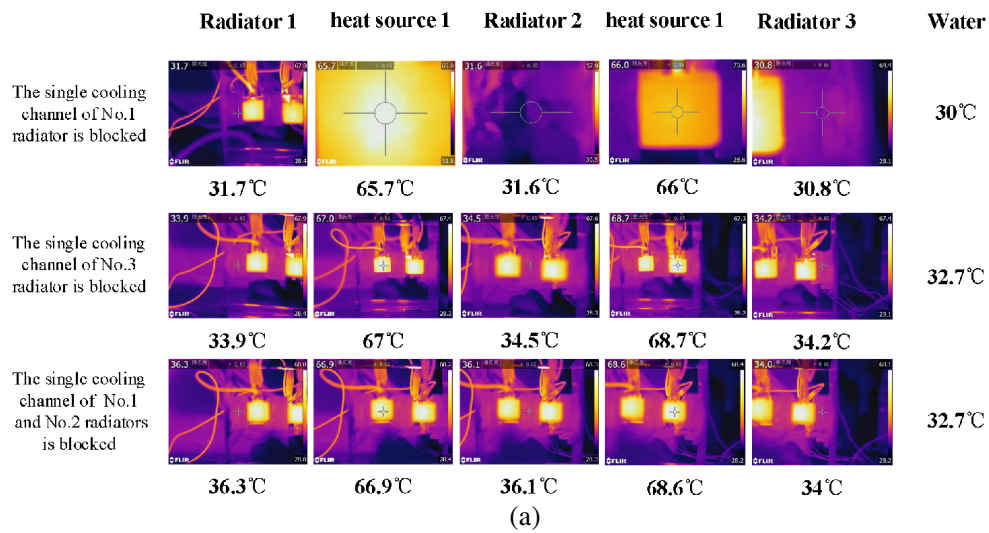
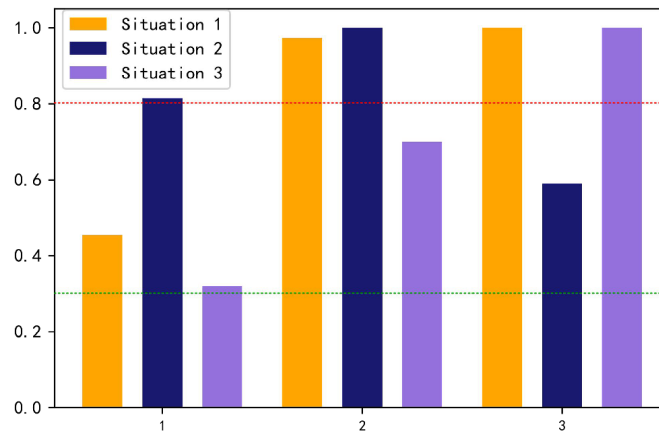


Figure 14. Schematic diagram of measuring points.



(a)



(b)

Figure 15. Temperature distribution and  $\langle W \rangle$  of test.

innerdiameter hoses, and cementresistances.

Since there are already infrared cameras in the valve hall of the converter valve, in order to ensure the usability of the method in engineering, an FIRL infrared camera is used to monitor the temperature in the test.

The heat source is cement resistance with resistance value of  $1\ \Omega$ . The electric energy is converted into Joule heat, and the flow rate of the water pump is 80 L/h. In the test, Three different cases of faults are set. The temperature measuring points are the red points in Fig. 14.

As shown in Fig. 15, the temperature data of different radiators and heat sources are recorded by the infrared camera and then brought into formula (3.6) to obtain  $\langle W \rangle$  of radiator.

From the comprehensive test 1 and test 2, as long as the geometries of the selected measuring points are the same, the blockage of the radiator can be described by  $\langle w \rangle$ . The experiment shows that the method is feasible in detecting the blockage of the radiator of the converter valve.

#### 4. CONCLUSION

The scaling of the equalizing electrode is more critical with the blocking of many converter stations, such as the Tianguang converter station. The research content of this paper is divided into two parts.

The first part: Based on the flow temperature field, the influence of radiator blockage on cooling system heat dissipation is analyzed. The results show that the radiator can still ensure that the valve group temperature is under the alarm threshold for partial blockage, a potentially dangerous state. Furthermore, for this potential hazard, a method of risk assessment of blocking radiator is proposed. The reliability theory is used to evaluate the risk of radiator blockage. Based on the structure-function and scaling action vector, the valve group tolerance index  $\psi$  and risk probability index  $\theta$  are calculated.

The second part: according to the pressure connection structure of the radiator and thyristor, the heat circuit model of the valve group is established. Furthermore, the relationship between blockage and valve unit temperature second-order differential  $U$  and  $T_{\text{water}}$  is deduced. The heat dissipation efficiency coefficient  $\langle W \rangle$  is used to evaluate the blockage of the radiator, and the simulation model and actual model verify the blocking monitoring theory.

According to the actual needs of the project, the infrared monitoring image in the valve hall of the current flow valve can be used. Combining the two methods can realize the online judgment of blockage and the assessment of heat dissipation risk of the valve, and ensure the safety of the operation of the flow change valve.

#### REFERENCES

1. Jackson, P. O. and B. Abrahamsson, "Corrosion in HVDC valve cooling systems," *IEEE Transactions on Power Delivery*, Vol. 12, No. 2, 1049–1052, 1997.
2. Jiang, Y., "Deposition behavior of corrosion products in inner cooling water system of HVDC converter valve," School of Environmental Science and Engineering, 2018.
3. Cheng, J., B. Wu, W. Mao, et al., "Failure statistics and countermeasures of UHVDC converter stations," *High Voltage Apparatus*, Vol. 54, No. 12, 292–298, 2018.
4. Xu, J., "Development of remote monitoring and intelligent maintenance system for pure water cooling device of HVDC transmission," Guangdong University of Technology, 2015.
5. Jiang, H., B. Zhai, X. He, et al., "Reliability evaluation of HVDC converter valve cooling system," *Power Safety Technology*, Vol. 16, No. 5, 60–63, 2014.
6. Yang, C., A. Wu, J. Li, and T. Ye, "Monitoring control and application of main pump in cooling system of flow changing valve," *Guangdong Chemical Industry*, 2020.
7. Ding, D., K. Zuo, Y. Gu, X. Liu, S. Sun, and J. Wu, "Analysis of equalizing electrode deposit in converter valve and it's removal methods," *Cleaning World*, Vol. 30, No. 6, 15–19, 2014.
8. Yang, F., T. He, B. Gao, B. Luo, L. Liu, and H. Luo, "Evaluation method of voltage-equalizing ability of electrodes in valve cooling systembased on sediment dynamic deposition model," *Electric Power Automation Equipment*, Vol. 40, No. 7, 188–197, 2020.

9. Lips, H. P., "Water cooling of HVDC thyristor valves," *IEEE Transactions on Power Delivery*, Vol. 9, No. 4, 1830–1837, 2002.
10. Wang, Y., Z. Hao, and R. Lin, "Primary analysis on corrosion and deposit in valve cooling system of tian-guang HVDC project," *High Voltage Engineering*, Vol. 9, 80–83, 2006.
11. Lou, Y., N. Liu, and J. Wang, "Comparative analysis on grading design of two different structural HVDC converter valve," *High Voltage Apparatus*, Vol. 52, No. 10, 153–157, 2016.
12. Fu, Z., "Series voltage equalization of silicon controlled valves for HVDC transmission," *High Voltage Apparatus*, Vol. 4, 24–30, 1976.
13. He, T., B. Gao, F. Yang, X. Song, Y. Cheng, and C. Liu, "The dynamic deposition behavior of grading electrode in converter valve cooling system considering electro-velocity-mass transfer field," *Transactions of China Electrotechnical Society*, Vol. 34, No. 14, 2863–2873, 2019.
14. Jin, C. and Y. Hong, "The conductivity of  $\text{La}\beta\text{-Al}_2\text{O}_3$ ," *Journal of the Chinese Ceramic Society*, Vol. 2, 3–5, 1998.
15. Wu, S., "Measurement of electronic conductivity in a second phase material-doped  $\beta$  alumina," *Journal of Tian Jin University*, Vol. 3, 114–122, 1985.
16. Li, X. and B. Yu, "Determination of conductivity and activation energy of polycrystalline  $\beta$ -alumina solid electrolyte," *Physics*, Vol. 1, 1–5, 1980.
17. Zhang, X., Z. Ren, and F. Mei, *Heat Transfer*, 5th Edition, China Construction Industry Press, 2007.
18. Hayat, T., T. Muhammad, S. A. Shehzad, et al., "Similarity solution to three dimensional boundary layer flow of second grade nanofluid past a stretching surface with thermal radiation and heat source/sink," *Aip Advances*, Vol. 5, No. 1, 1326–1336, 2015.
19. Kong, X. and C. Wang, *Application of Finite Element Method in Heat Transfer*, Science Press, 1981.
20. Xing, X.-K., C.-F. Ma, Y.-C. Chen, and L. Song, "An improved method for measuring and inspecting thermal resistance of scale in tube by temperature difference," *Journal of the University of Petroleum*, Vol. 5, 70–73, China, 2004.
21. Zhang, C., "Study on the scaling monitoring of circulating water and the treatment of organic wastewater," Huazhong University of Science and Technology, 2011.
22. Tao, W., *Numerical Heat Transfer*, Xi'an Jiaotong University Press, 2001.
23. Yao, G., H. Yu, and X. Zheng, "Research on the scaling inspection technology of organic heat transfer material boiler under active temperature difference excitation," *Safety of Special Equipment in China*, Vol. 31, No. 10, 15–18, 2015.
24. Cao, J. and K. Cheng, *Introduction to Reliability Mathematics: Revised Edition*, Higher Education Press, 2006.
25. Hong, Y. and T. Yu, "Reliability improvement strategies for HVDC transmission system," *Energy & Power Engineering*, Vol. 5, No. 3, 52–56, 2013.
26. Zhang, X., Y. Liu, and S. Ma, "Meshfree methods and their applications," *Advances in Mechanics*, Vol. 39, No. 1, 1–36, 2009.
27. Jin, C., J. Liu, and B. Zhang, "Inverse problems for PDEs: Models, computations and applications," *Scientia Sinica Mathematica*, Vol. 49, No. 4, 3–26, 2019.
28. Schuster, T., B. Kaltenbacher, B. Hofmann, et al., *Regularization Methods in Banach Spaces*, De Gruyter, 2012.
29. Li, M. and X. Li, "Application research on quality evaluation of urban human settlements based on the BP network improved by GA," *Economic Geography*, Vol. 1, 99–103, 2007.
30. Wu, S., "Optimization research of BP neural network and genetic algorithm based on numerical calculation method," Yunnan Normal University, 2006.
31. Zhang, W., F. Zheng, L. Hao, et al., "Corrosion characteristics of aluminum radiator for valve cooling system based on constant potential method," *High Voltage Apparatus*, Vol. 55, No. 5, 175–181, 2019.

32. De, D., “HVDC Valve internal cooling system corrosion and scaling mechanism and protection technology research,” Xi’an University of Technology, 2017.
33. Yin, L., Y. Jin, C. Leygraf, et al., “A FEM model for investigation of micro-galvanic corrosion of Al alloys and effects of deposition of corrosion products,” *Electrochimica Acta*, 310–318, 2016.
34. Huang, H., T.-H. Liao, S. B. Kim, X. Xu, L. Tsang, T. J. Jackson, and S. Yueh, “L-band radar scattering and soil moisture retrieval of wheat, canola and pasture fields for smap active algorithms,” *Progress In Electromagnetics Research*, Vol. 170, 129–152, 2021.
35. Fornieri, A., M. J. Martínez-Pérez, and F. Giazotto, “Electronic heat current rectification in hybrid superconducting devices,” *Aip Advances*, Vol. 5, No. 5, 15, 2015.
36. Xu, H., J. Zhu, L. Tsang, and S. B. Kim, “A fine scale partially coherent patch model including topographical effects for GNSS-R Ddm simulations,” *Progress In Electromagnetics Research*, Vol. 170, 97–128, 2021.
37. Weon, B. M., J. H. Je, and C. Poulard, “Convection-enhanced water evaporation,” *AIP Advances*, Vol. 1, 1, 2011.